Journal of Magnetism and Magnetic Materials 421 (2017) 393–402

Contents lists available at ScienceDirect

Journal of Magnetism and Magnetic Materials

journal homepage: www.elsevier.com/locate/jmmm

Magnetic properties of nickel halide hydrates including deuteration effects

G.C. DeFotis [a,*], M.J. Van Dongen [a], A.S. Hampton [a], C.H. Komatsu [a], K.T. Trowell [a], K.C. Havas [a], C.M. Davis [a], C.L. DeSanto [a], K. Hays [b], M.J. Wagner [b]

[a] Chemistry Department, College of William & Mary, Williamsburg, VA, 23187 United States
[b] Chemistry Department, George Washington University, Washington, DC, 20052 United States

ARTICLE INFO

Article history:
Received 4 May 2016
Received in revised form
18 July 2016
Accepted 10 August 2016
Available online 11 August 2016

Keywords:
Antiferromagnet
Magnetic susceptibility
Exchange interactions
Heisenberg model
Magnetic transition
Powder X-ray diffraction

ABSTRACT

Magnetic measurements on variously hydrated nickel chlorides and bromides, including deuterated forms, are reported. Results include locations and sizes of susceptibility maxima, T_{max} and χ_{max}, ordering temperatures T_c, Curie constants and Weiss theta in the paramagnetic regime, and primary and secondary exchange interactions from analysis of low temperature data. For the latter a 2D Heisenberg model augmented by interlayer exchange in a mean-field approximation is applied. Magnetization data to 16 kG as a function of temperature show curvature and hysteresis characteristics quite system dependent. For four materials high field magnetization data to 70 kG at 2.00 K are also obtained. Comparison is made with theoretical relations for spin-1 models. Trends are apparent, primarily that T_{max} of each bromide hydrate is less than for the corresponding chloride, and that for a given halide nD_2O ($n=1$ or 2) deuterates exhibit lesser T_{max} than do nH_2O hydrates. A monoclinic unit cell determined from powder X-ray diffraction data on $NiBr_2 \cdot 2D_2O$ is different from and slightly larger than that of $NiBr_2 \cdot 2H_2O$. This provides some rationale for the difference in magnetic properties between these.

1. Introduction

Hydrated 3d transition metal chlorides are a very important class of insulating magnets. Many examples, in particular among the common hydration forms di-, tetra- and hexahydrate, have served as notable examples of definite magnetic model systems, e.g., three-dimensional Heisenberg antiferromagnet [1,2]. So it is somewhat surprising that corresponding bromide materials are much less thoroughly studied. Potentially fruitful comparisons of, for example, exchange interactions via metal ion-(di)halide-metal ion pathways could emerge.

In order to further such examination we report here susceptibility and magnetization data on $NiBr_2{\cdot}2H_2O$ and $NiBr_2{\cdot}H_2O$. $NiCl_2{\cdot}2H_2O$ is characterized by linear chains of chloride bibridged metal ions, with slightly less than 90° Cl–Ni–Cl bridging angles [3]. Slight relative tilting of adjacent $NiCl_4$ planar coordination units along the chain leads to a repeat unit of two nickel centers. Crystallization is in a monoclinic $C2/m$ structure, with $NiCl_2NiCl_2Ni\ldots$ chains along the b axis. Chains are coupled structurally by hydrogen bonding. The unit-cell volume per formula unit is 105.0 Å^3. $NiCl_2 \cdot 2H_2O$ is a nearly isotropic 3D Heisenberg antiferromagnet ordering at 7.25 K, with a spin reorientation transition at 6.31 K [4,5]. The spins in each $NiCl_2NiCl_2Ni\ldots$ chain are ferromagnetically aligned along a^*, normal to both b and c. Spins of chains separated by $\pm(a \pm c)/2$ are oppositely directed to give overall antiferromagnetism. A metamagnetic transition occurs at 19 kG near 0 K, followed by transitions at 56 and 82 kG, to states of increasing ferromagnetic alignment. Spins are very nearly along metal-oxygen bonds, which are essentially normal to the $MCl_2MCl_2M\ldots$ chains. Strong ferromagnetic intrachain and somewhat weaker but still significant antiferromagnetic interchain exchange interactions exist.

The only other $NiX_2 \cdot nH_2O$ ($n=1$ or 2) structure determined, only partially, is that of $NiBr_2 \cdot 2H_2O$ [6]. The unit cell is isomorphic with that of the chloride, in monoclinic space group $I2/m$ with $Z=4$. Lattice parameters are from 3.8% to 5.0% larger in the bromide; these are $a=7.21(1)$ and 6.9093(5) Å, $b=7.23(1)$ and 6.8858 (6) Å, and $c=9.17(1)$ and 8.8298(4) Å for $NiBr_2 \cdot 2H_2O$ and $NiCl_2 \cdot 2H_2O$ respectively, with $\beta=92.4(3)°$ and 92.246(2)° in the same order. Heat capacity data indicate successive magnetic transitions occurring at 6.23 and 5.79 K, presumably analogous to those in the chloride but at somewhat lower temperatures [7].

Another point of major interest arises. The effects of deuteration on the magnetic properties of transition metal compounds containing hydrogen, including those with waters of hydration, are

* Corresponding author.
E-mail address: gxdefo@wm.edu (G.C. DeFotis).

http://dx.doi.org/10.1016/j.jmmm.2016.08.043
0304-8853/

typically quite small, though the literature is not extensive. This need not necessarily be the case however, since such effects are a function of structural details, especially if coordinated waters provide important superexchange pathways. Our report on $MnCl_2 \cdot D_2O$ and $CoCl_2 \cdot D_2O$ is a significant recent example [8]. Therefore we also prepare and examine each D_2O containing nickel chloride and nickel bromide hydration form. Significant contrasts with the H_2O containing materials appear, somewhat more pronounced for bromides than for chlorides.

2. Experimental

2.1. Preparation and characterization

Both $NiCl_2 \cdot 2H_2O$ and $NiCl_2 \cdot H_2O$ were studied previously, by others and by us [4,5,9]. The former was prepared in polycrystalline form, for comparison with the other materials reported here, by slow evaporation of an aqueous solution of $NiCl_2$ at 75 °C. A higher temperature of ~110 °C was needed to obtain monohydrate. Grinding of the materials, followed by a brief period of similar heat treatment, in order to eliminate any occluded water, led to uniform fine-grained solids, light green and medium yellow respectively. Thermogravimetric analysis confirmed that the desired hydrate was obtained, to within 0.05 water unit. This is similar precision as for many other transition metal halide hydrates studied by us previously.

Preparation of $NiBr_2 \cdot 2H_2O$ and $NiBr_2 \cdot H_2O$ proceeded in analogous fashion, dissolving high purity anhydrous nickel dibromide in deionized water followed by slow evaporation to dryness. A temperature of ~80 °C, very similar to that in a prior report on the heat capacity of this substance [7], yielded $NiBr_2 \cdot 2H_2O$. For previously unreported $NiBr_2 \cdot H_2O$, a temperature of ~90 °C was found by trial and error to suffice. This is significantly less than that needed to obtain the chloride monohydrate. The colors of the two bromide hydrates were a similar dark yellow. Thermogravimetric analysis confirmed the hydration states to within 0.05 water unit.

Preparation and hydration state analysis of $NiCl_2 \cdot 2D_2O$, $NiCl_2 \cdot D_2O$, $NiBr_2 \cdot 2D_2O$ and $NiBr_2 \cdot D_2O$ occurred similarly. High purity anhydrous halides were dissolved in fully deuterated D_2O (99.8%, Acros Chemicals) in a glove box, then placed in a vacuum oven filled with Ar(g) for evaporation, in order to avoid contamination by atmospheric water vapor. In the absence of literature guidance a trial and error process was required in order to find appropriate temperatures for obtaining these materials. Somewhat higher temperatures than for the H_2O containing systems were needed: ~108 °C, ~138 °C, ~88 °C and ~95 °C in the same order as above. The colors of the solids were a similar light yellow for the two chlorides, slightly darker yellow for $NiBr_2 \cdot 2D_2O$, and somewhat darker yellow for $NiBr_2 \cdot D_2O$. Thermogravimetric analysis confirmed the target hydration states to within 0.05 D_2O unit.

2.2. Magnetic measurements

Magnetization and susceptibility measurements were made with a variable temperature vibrating sample magnetometer system. The data shown are field cooled measurements and are corrected for the (rather small) effects of diamagnetism and demagnetization and the even smaller sample holder contribution. Applied magnetic fields in susceptibility measurements ranged from 100 G to 1 kG depending on the temperature. No field dependence of the susceptibility was apparent, as expected for such relatively small field values. Polycrystalline samples of approximately 100 mg size were packed into nonmagnetic sample holders under dry conditions, weighed accurately, and screwed onto a nonmagnetic sample rod in immediate proximity to a calibrated Cernox resistance thermometer. Temperatures are accurate to $\pm 0.005 - 0.5$ K depending on the range. Magnetic field values are accurate to $\pm$ max (2 G, 0.1%), and magnetization and susceptibility data to 1.5% absolute, with substantially better precision. In handling of the materials, care was taken to minimize exposure to atmospheric water vapor.

2.3. Powder X-ray diffraction

In preparing samples for X-ray diffraction a nitrogen filled glove bag was purged twice and a small dewar of liquid nitrogen evaporating in it in order to minimize humidity before opening storage vials. An agate mortar and pestle was used to grind and mix a few milligrams of each sample with a drop of Paratone™ oil, which was then spread onto a zero-diffraction quartz plate and transferred in an air-free container to a Rigaku Miniflex+ powder X-ray diffractometer (Cu K-alpha) housed inside a nitrogen filled glove box (Mbraun UNIlab™). Scans were acquired at 10 data points per degree from 10 to 90 degrees 2-theta at a rate of 1° per minute.

Jade 6.1™ was used to perform background correction, K-alpha 2 removal, and peak finding on the diffraction data. Peaks with a height of 2% or greater relative to the maximum peak height in the diffraction pattern were used for cell indexing. Cell indexing was completed using McMaille (version 4) software [10].

3. Measurements and analysis

3.1. Magnetic susceptibility

3.1.1. Paramagnetic regime

The inverse molar magnetic susceptibilities of $NiCl_2 \cdot 2D_2O$ and $NiCl_2 \cdot D_2O$ appear in Fig. 1. Data are corrected for diamagnetism and demagnetization, both quite small, and a Van Vleck T-independent contribution. The latter is estimated from [11] $\chi_{VV}=(N_o\mu_B{}^2/\lambda)$ (2-g) with effective spin-orbit coupling constant $\lambda=-270\ cm^{-1}$ (better for octahedral Ni^{2+} than free-ion $-315\ cm^{-1}$) and an initial g value from a fit prior to applying the correction. Fairly good linearity is apparent above 50 K and 70 K for the $2D_2O$ and D_2O materials respectively. Curie–Weiss form,

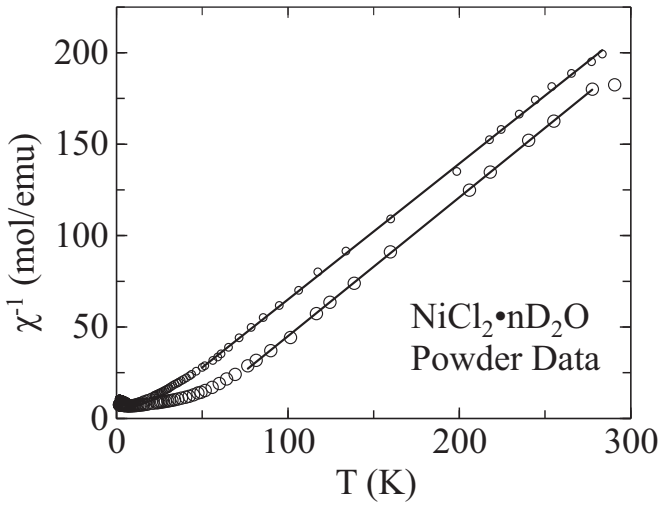

Fig. 1. Inverse molar magnetic susceptibilities vs. temperature for $NiCl_2 \cdot 2D_2O$ (small circles) and $NiCl_2 \cdot D_2O$ (large circles). Also shown are Curie–Weiss fits described in text.